

Gravitational Lensing by Wormholes

Juan Manuel Tejeiro S.¹ and Eduard Larranaga²

^{1,2}*Observatorio Astronomico Nacional. Universidad Nacional de Colombia*

June 8, 2022

Abstract

Natural wormholes and its astrophysical signatures have been suggested in various opportunities. By applying the strong field limit of gravitational lensing theory, we calculate the deflection angle and magnification curves produced by Morris-Thorne wormholes in asymptotically flat space-times. The results show that wormholes act like convergent lenses. Therefore, we show that it is hard to distinguish them from black holes using the deflection's angle of the gravitational lens effect, in contrast with the results reported by Cramer et.al. and Safanova et.al. However, we also show that it is possible, in principle, distinguish them by the magnification curves, in particular, by observing the position of the peak of the Einstein's ring.

1 Introduction

Wormholes are space-time regions with two mouths connected by a throat. Since the mouths are not hidden by event horizons and there is no singularity inside, wormholes permit the passage of massive particles or photons from one side to the other. Morris and Thorne[1, 2] shown that wormholes require the violation of the averaged null energy condition in order to satisfy the Einstein field equations in the throat. Thus, matter in this region must exert gravitational repulsion to make a stable configuration. The study of these solutions lead to an interesting question: May some observable electromagnetic signatures give the possibility of wormhole identification?

One of the most important applications of General Relativity is Gravitational Lensing. Since matter inside the wormhole antigravitate, Cramer et. al. [5] and Safanova et. al. [6] have studied the lensing effects of negative masses on light rays from point sources in the background, and argued that this will be the effect produced by natural stellar-size wormholes. The study of lensing effects show that positive masses acts like convergent lenses, while the study of Safanova et. al. for negative masses show that these act basically like divergent

lenses. This means that the deflection angle is negative (divergent). Therefore, light from a point source will be concentrated on the border of an *umbra region*, producing two intensity enhancements: one before and one after the occultation event.

Recently, the scientific community started to look gravitational lensing from a strong field perspective. This limit refers to the effect produced by a very massive object and/or when the light rays that are affected pass very close to the lens. Bozza [7] provided an analytic method to calculate the deflection angle for any spherically symmetric spacetime in the strong field limit, and one important result of this is that a light ray with a very small impact parameter will wind one or several times around the lens before emerging, producing an infinite set of *relativistic images*.

In this paper, we will use the method of Bozza to calculate a more realistic lensing effect of Morris-Thorne wormholes, and it will permit us to show that wormhole spacetimes present a *positive deflection angle*, i.e. wormholes does not act like divergent lenses in the general case. This means that exotic matter needed to construct the solutions does not have a direct observable signature for an outside observer.

In section II we give the metric of the studied wormhole solutions, section III gives the essential knowledge about strong gravitational lensing as described by Bozza and in section IV we calculate the deflection angle for the presented wormholes. In section V we compare the obtained angles with the Schwarzschild's deflection angle and finally, in section VI we put some conclusions.

2 Morris-Thorne Wormholes

In the pionnering work of Morris and Thorne they describe a general class of solution of Einstein equations representing wormholes. The conditions that they impose in order to obtain the general form of the metric tensor include:

1. The metric must be spherically symmetric and static (independent of time)
2. The solution must have a throat joining two asymptotically flat regions of spacetime
3. The metric must satisfy Einstein equations in every point of spacetime
4. The geometry will not have event horizons nor singularities

Under these, the general form for the metric tensor is

$$ds^2 = -e^{2\Phi(r)} c^2 dt^2 + \frac{1}{1 - \frac{b(r)}{r}} dr^2 + r^2 (d\theta^2 + \sin^2\theta d\phi^2), \quad (1)$$

where $\Phi(r)$ is the redshift function and $b(r)$ is the form function. When imposing condition 3 above, we obtain the relation between the functions $\Phi(r)$ and $b(r)$ and the stress-energy tensor that produces the wormhole spacetime

geometry. Outside the wormhole, the spacetime is considered asymptotically flat and have a line element given by Schwarzschild metric,

$$ds^2 = - \left(1 - \frac{2GM}{r^2}\right) dt^2 + \left(1 - \frac{2GM}{r^2}\right)^{-1} dr^2 + r^2 (d\theta^2 + \sin^2\theta d\phi^2). \quad (2)$$

The junction conditions that follow from the theory of general relativity are the continuity of the metric components and the extrinsic curvature across the surface of juncture.

To obtain specific solutions, in wormhole studies is usual to fix a spacetime geometry (i.e. to fix the functions Φ and b in order to obtain a wormhole geometry) and then use the Einstein equations to derive the matter distribution needed to obtain the respective metric. Following [1, 2] is easy to see that many wormhole geometries need *exotic matter* (i.e. matter that does not obey the null energy condition) to exist, and it is localized at the throat of the wormhole. This need is what led Cramer et. al. [5] and Safanova et. al. [6] to model a wormhole as a point of negative mass to study gravitational lensing.

2.1 Specific Solutions

In this paper we will consider only two specific wormhole solutions obtained by Lemos et. al. [4]. In both cases we will define r_m as the radius of the throat and a as the radius of the mouth of the wormhole.

2.1.1 Solution A

The first solution has an interior metric ($r_m \leq r \leq a$) given by

$$ds^2 = - \left(1 - \sqrt{\frac{r_m}{a}}\right) dt^2 + \frac{dr^2}{\left(1 - \sqrt{\frac{r_m}{r}}\right)} + r^2 (d\theta^2 + \sin^2\theta d\phi^2), \quad (3)$$

and an exterior metric ($a < r < \infty$) given by

$$ds^2 = - \left(1 - \frac{\sqrt{r_m a}}{r}\right) dt^2 + \frac{dr^2}{\left(1 - \frac{\sqrt{r_m a}}{r}\right)} + r^2 (d\theta^2 + \sin^2\theta d\phi^2). \quad (4)$$

Since the exterior solution must represent Schwarzschild metric, we can associate a mass to the wormhole,

$$M = \frac{\sqrt{r_m a}}{2G}, \quad (5)$$

and as can be seen, the complete metric is smoothly joined at mouth radius a .

2.1.2 Solution B

The second solution has an interior metric ($r_m \leq r \leq a$) given by

$$ds^2 = - \left(1 - \left(\frac{r_m}{a} \right)^2 \right) dt^2 + \frac{dr^2}{\left(1 - \left(\frac{r_m}{r} \right)^2 \right)} + r^2 (d\theta^2 + \sin^2\theta d\phi^2), \quad (6)$$

and an exterior metric ($a < r < \infty$) given by

$$ds^2 = - \left(1 - \frac{r_m^2}{ar} \right) dt^2 + \frac{dr^2}{\left(1 - \frac{r_m^2}{ar} \right)} + r^2 (d\theta^2 + \sin^2\theta d\phi^2). \quad (7)$$

Again, the metric is smoothly joined at mouth radius a , and since the exterior solution must represent Schwarzschild metric, we associate a mass to the wormhole,

$$M = \frac{r_m^2}{2aG}. \quad (8)$$

Both metrics represent wormholes connecting two asymptotically flat spacetimes, and to both of them we associate a positive external mass. This fact inspires us to think that a light ray that passes near the wormhole but not into it, will have a deflection similar to that produced by a Schwarzschild geometry, while a light ray that goes into the wormhole will have a little different behavior.

3 Gravitational Lensing

Because of the arguments given in the preceding section, the gravitational lensing effects produced by a wormhole will be similar to those produced by a Schwarzschild metric when the deflected light ray does not enter into the wormhole, but in order to obtain a mathematical expression for the deflection angle of a light ray passing very close to the wormhole we will use the analytical method for strong field limit gravitational lensing of Bozza [7].

We consider the geometry as follows: A light ray from a source (S) is deflected by the wormhole acting as a lens (L) and reaches the observer (O). The background spacetime is asymptotically flat. The line joining lens and observer (OL) is the optic axis. β and θ are the angular position of the source and the image with respect to the optical axis, respectively. The distances between observer and lens, lens and source, and observer and source are D_{OL} , D_{LS} and D_{OS} , respectively.

The relation between the position of the source and the position of the image is called the *lens equation*[8],

$$\tan\theta - \tan\beta = \frac{D_{LS}}{D_{OS}} [\tan\theta + \tan(\alpha - \theta)], \quad (9)$$

where α is the deflection angle. For a spherically symmetric spacetime with line element

$$ds^2 = -A(x) dt^2 + B(x) dx^2 + C(x) (d\theta^2 + \sin^2\theta d\phi^2), \quad (10)$$

the deflection angle was obtained by Virbhadra et. al. [9] as a function of closest approach $x_o = \frac{r_o}{2M}$ as

$$\alpha(x_o) = I(x_o) - \pi, \quad (11)$$

where

$$I(x_o) = \int_{x_o}^{\infty} \frac{2\sqrt{B(x)}dx}{\sqrt{C(x)}\sqrt{\frac{C(x)A(x_o)}{C(x_o)A(x)} - 1}}. \quad (12)$$

The method of Bozza is to expand the integral in $I(x_o)$ around the photon sphere to obtain a logarithmic expression for $\alpha(x_o)$, and then, by using the lens equation, obtain the position of the produced images.

4 Deflection Angle for Wormholes

The way to calculate the deflection angle produced by a wormhole depends on the closest approach of the light ray:

4.1 Closest Approach outside Wormhole's Mouth

When the closest approach of the light ray is greater than wormhole's mouth ($r_o \geq a$), the deflection angle is produced only by the external metric. Therefore, the lensing effect is, in this case, exactly the same as the produced by a Schwarzschild metric with the correspondent mass. This angle is given [7] by

$$\alpha(x_o) = -2\ln\left(\frac{2x_o}{3} - 1\right) - 0.8056. \quad (13)$$

4.2 Closest Approach inside Wormhole's Mouth

Since wormhole solutions described above are defined in two regions, when the closest approach of the light ray is inside wormhole's mouth ($r_m < r_o < a$), the deflection angle must be calculated as two contributions: first a deflection produced by the external Schwarzschild-like metric, and second the contribution produced by the internal metric.

In both of the specific solutions given, the external contribution to the deflection angle is given as Schwarzschild deflection above but with a closest approach equal to the wormhole's mouth,

$$\alpha_e = -2\ln\left(\frac{2a}{3} - 1\right) - 0.8056. \quad (14)$$

The contribution of the internal metric has to be calculated for each solution:

4.2.1 Solution A

For the specific solution A described above we have

$$I_A(x_o) = 2 \int_{x_o}^a \frac{1}{\sqrt{x^2 \left(1 - \sqrt{\frac{x_m}{x}}\right)} \sqrt{\frac{x^2}{x_o^2} - 1}} dx. \quad (15)$$

Making the change $y = \frac{x}{x_o}$ we obtain

$$I_A(x_o) = 2 \int_1^{\frac{a}{x_o}} \frac{1}{\sqrt{y^2 \left(1 - \sqrt{\frac{x_m}{x_o y}}\right)} \sqrt{y^2 - 1}} dy. \quad (16)$$

The integrand diverges for $y = 0$, $y = \frac{x_m}{x_o}$ and $y = 1$. However, only the third of these values is in the integration range. Because of this, we will expand the argument of the square root around this divergence up to the second order in y . This gives

$$I_A(x_o) = 2 \int_0^{\frac{a}{x_o} - 1} \frac{dz}{\sqrt{\zeta_A z + \eta_A z^2}}, \quad (17)$$

where

$$z = y - 1 \quad (18)$$

$$\zeta_A = 2 \left(1 - \sqrt{\frac{x_m}{x_o}}\right) \quad (19)$$

$$\eta_A = 2 \left(5 - 4\sqrt{\frac{x_m}{x_o}}\right). \quad (20)$$

When ζ_A is non-zero, the leading order of the divergence is $z^{1/2}$, which can be integrated to give a finite result. When ζ_A vanishes, the divergence is z^{-1} which makes the integral to diverge. In this way, the condition $\zeta_A = 0$ gives us the radius of the photon sphere,

$$x_{ps} = x_m. \quad (21)$$

This means that any photon with a closest approach distance $x_o = x_m$ will be captured and it is interesting to note that the radius of the photon sphere does correspond to the throat radius. Therefore, any photon with a closest approach distance less than the throat radius does not emerge in the same part of the universe, but goes into the wormhole to the other mouth.

Integral in (17) can be exactly made as

$$I_A(x_o) = -\frac{2}{\sqrt{\eta_A}} \ln \left[\frac{\zeta_A}{\zeta_A + 2\eta_A \left(\frac{a}{x_o} - 1\right) + 2\sqrt{\eta_A \left(\frac{a}{x_o} - 1\right)} \left(\zeta_A + \eta_A \left(\frac{a}{x_o} - 1\right)\right)} \right]. \quad (22)$$

The total deflection angle for solution A is then

$$\alpha_A(x_o) = \alpha_e + I_A(x_o). \quad (23)$$

4.2.2 Solution B

For the specific solution B, we have

$$I_B(x_o) = 2 \int_{x_o}^a \frac{1}{\sqrt{x^2 \left(1 - \frac{x_m^2}{x^2}\right)} \sqrt{\frac{x^2}{x_o^2} - 1}} dx. \quad (24)$$

This integral can be rewritten as

$$I_B(x_o) = 2 \int_1^{\frac{a}{x_o}} \frac{dy}{\sqrt{y^2 \left(1 - \frac{x_m^2}{x_o^2 y^2}\right)} (y^2 - 1)}, \quad (25)$$

where $y = \frac{x}{x_o}$. Once more, the integrand diverges for $y = 0$, $y = \frac{x_m}{x_o}$ and $y = 1$, but we will consider only the third of these values. Expanding the argument of the square root around this divergence up to the second order in y we have

$$I_B(x_o) = 2 \int_0^{\frac{a}{x_o} - 1} \frac{dz}{\sqrt{\zeta_B z + \eta_B z^2}}, \quad (26)$$

where this time

$$z = y - 1 \quad (27)$$

$$\zeta_B = 2 \left(1 - \frac{x_m^2}{x_o^2}\right) \quad (28)$$

$$\eta_B = 2 \left(5 - \frac{x_m^2}{x_o^2}\right). \quad (29)$$

The condition $\zeta_B = 0$ gives us the radius of the photon sphere, and again we have

$$x_{ps} = x_m \quad (30)$$

Therefore the behavior of a photon near this radius is similar to the described before. The integral in (26) can be exactly made as

$$I_B(x_o) = -\frac{2}{\sqrt{\eta_B}} \ln \left[\frac{\zeta_B}{\zeta_B + 2\eta_B \left(\frac{a}{x_o} - 1\right) + 2\sqrt{\eta_B \left(\frac{a}{x_o} - 1\right) \left(\zeta_B + \eta_B \left(\frac{a}{x_o} - 1\right)\right)}} \right], \quad (31)$$

and the total deflection angle for solution B is

$$\alpha_B(x_o) = \alpha_e + I_B(x_o). \quad (32)$$

5 Comparison of deflection angles

As we have shown in the preceeding section, wormholes present an interesting lensing effect. Photons with a closest approach distance greater than wormhole's mouth have a Schwarzschild lensing effect, while photons with a closest approach distance less than wormhole's mouth have a Schwarzschild lensing plus an inner lensing effect. Because of this, is important to compare the deflection angle of wormholes with the deflection of Schwarzschild,

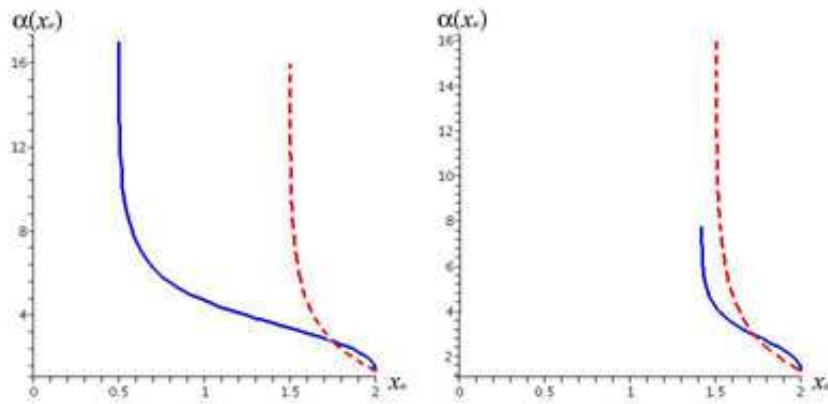


Figure 1. In the left side we have the deflection angle for the wormhole solution A (continuous) compared with Schwarzschild's deflection angle (dotted). Wormhole's mouth is at $a = 2$ (in Schwarzschild units), and the throat is at $x_m = \frac{1}{2}$. It is easy to see that the blue curve diverges at $x_o = x_m$. In the right side we have the deflection angle for the wormhole solution B (continuous) compared with Schwarzschild's deflection angle (dotted). Wormhole's mouth is again at $a = 2$ (in Schwarzschild units) and the throat is at $x_m = \sqrt{2}$. The blue curve diverges exactly at $x_o = x_m$. In both cases, outside wormhole's mouth the angles coincide.

From these graphics we can see that the deflection angle for light passing outside the wormhole is the same as the one produced by Schwarzschild, and some differences appear when light goes inside. One of the most important is the divergence in the blue curves: they occur exactly at wormhole's throat, showing that this surface corresponds to a photon sphere.

6 Magnification

Magnification is an important characteristic of Gravitational Lensing because it is easily observable. As is already known, magnification is given by

$$\mu = \frac{\sin\beta}{\sin\theta} \frac{d\beta}{d\theta}. \quad (33)$$

Then, in order to obtain the magnification produced by a wormhole we will use the produced deflection angle and, using the lens equation (9), obtain a relation between the angular positions of the image (θ) and the source (β). since the deflection angle is calculated for each of the presented solutions, the magnification must be evaluated also for each wormhole.

6.1 Solution A

For the first of the presented solutions the magnification is given by:

$$\mu = \left(1 - \frac{D_{ds}D_d}{D_s} \sqrt{1 - \sqrt{\frac{x_m}{a}} \frac{\alpha(x_o)}{x_o}} \right)^{-1} \left(1 - \frac{D_{ds}D_d}{D_s} \sqrt{1 - \sqrt{\frac{x_m}{a}} \frac{d\alpha}{dx_o}} \right)^{-1}, \quad (34)$$

where $\alpha(x_o)$ is the deflection obtained before and the derivative $\frac{d\alpha}{dx_o}$ can be evaluated using a math software. If we plot the magnification as a function of the closest approach we have the following curves.

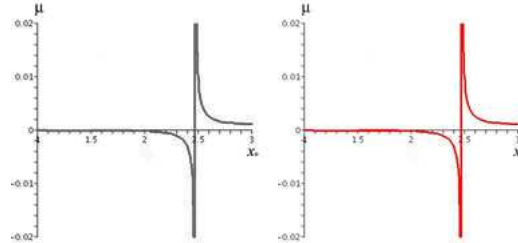


Figure 2. Comparison of the magnification for Schwarzschild's black hole (left) and wormhole A (right). At this scale the curves look the same. Wormhole's mouth is at $a = 2$

As it is easily seen, the two curves look exactly the same. Moreover, we can see the divergence that corresponds to the Einstein' ring as is expected because the mouth of the wormhole is situated inside this ring and the exterior metric is exactly the same as Schwarzschild's metric.

However if we made a zoom near the wormhole's mouth, we can see how in the wormhole's case, the magnification shows a discontinuity:

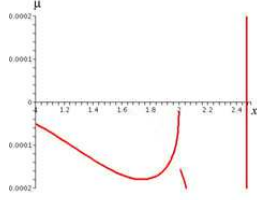


Figure 3. Zoom of the magnification for wormhole A, near its mouth located at $a = 2$

It is important to note that the discontinuity occurs exactly at the mouth of the wormhole, and it happens because here is where the matter distribution of the wormhole begins. It is also seen a little peak in the magnification curve inside the wormhole that is not seen in Schwarzschild geometry.

Moreover, when we change the wormhole's parameters, a very interesting behavior appears. In the next set of figures we can see the magnification curve for wormholes with different mouth sizes.

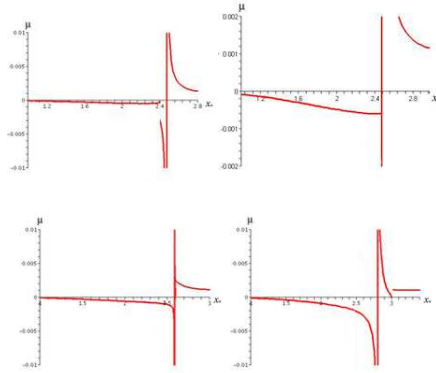


Figure 4. Magnification curves for wormhole A with different mouth's sizes. In the first we have $a = 2.4$, in the second $a = 2.47$, in the third $a = 2.6$ and in the fourth $a = 3$. Note that in each case we have a discontinuity at a .

It is easily seen, that when we change the mouth of the wormhole, the little peak inside grows. When the mouth of the wormhole is inside the Einstein's ring radius the magnification behaves just as commented before, but when the mouth of the wormhole is greater than the Einstein ring the peak in magnification of this ring disappears and there appears a new peak produced by the wormhole. Observationally, this fact shows an "Einstein's ring", shifted from the original position and this effect can be, in principle, measured.

6.2 Solution B

For wormhole B we obtain a magnification given by the expression

$$\mu = \left(1 - \frac{D_{ds}D_d}{D_s} \sqrt{1 - \frac{x_m^2}{a^2}} \frac{\alpha(x_o)}{x_o}\right)^{-1} \left(1 - \frac{D_{ds}D_d}{D_s} \sqrt{1 - \frac{x_m^2}{a^2}} \frac{d\alpha}{dx_o}\right)^{-1}. \quad (35)$$

Again, we have here the deflection angle for solution B, $\alpha(x_o)$ and the derivative $\frac{d\alpha}{dx_o}$, that is evaluated using a math software. If we plot the magnification as a function of the closest approach x_o , the curve looks exactly the same as the Schwarzschild magnification (just as for the wormhole solution a in Figure 2.). However, when we make a zoom of the region near wormhole's mouth we get a little difference:

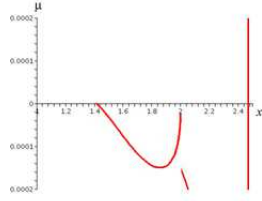


Figure 5. Zoom of the magnification for wormhole B, near its mouth located at $a = 2$

See how we have again a discontinuity localized at the wormhole's mouth and a little peak inside the wormhole that makes the difference when compared with Schwarzschild's geometry. Just as in the specific solution B, the inside peak's position depends on the size of the wormhole's mouth. This fact is shown in the next set of figures:

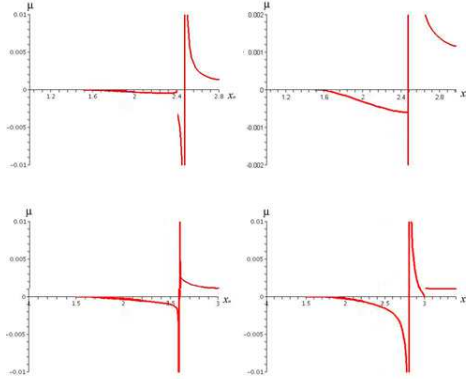


Figure 6. Magnification curves for wormhole B with different mouth's sizes. In the first we have $a = 2.4$, in the second $a = 2.47$, in the third $a = 2.6$ and in the fourth $a = 3$. Note that in each case we have a discontinuity at a .

Again it is seen an observational difference in the magnification because there is a peak that does not correspond exactly to the Einstein's ring but to the wormhole with a sufficiently greater mouth.

7 Conclusion

Gravitational lensing is one of the most important effects in General Relativity. In this paper we have applied the strong field lensing method to Morris-Thorne wormholes and the analysis of the deflection angle and magnification produced by the two specific wormhole solutions described show that the behaviour of these objects is very similar to the behaviour of Schwarzschild's solution. As can be seen from the graphics, there is a logarithmic divergence of the deflection angle, and there is a photon sphere that corresponds to the throat of the wormhole. This behavior contrast with the behaviour reported by Cramer et. al. [5] and Safanova et. al. [6] since their model for the wormhole is a negative punctual mass. Although the two solutions considered here need some exotic (gravitationally negative) mass inside, the behavior of light deflection does not differ significantly from the Schwarzschild case.

On the other side, magnification curves for the wormholes are similar to the obtained for Schwazschild, but when looking in some detail, there is a discontinuity in the curve (at the point where the mass distribution begins). It is also of great importance to note here that the size of the mouth of the wormhole affects the behavior of the magnification curve, and specially when the mouth of the wormhole is greater than the size of the Einstein's ring. In this last case we see how a ring appears but it is not at the expected position for the Einstein's ring, making a possible way to identify wormholes from other mass distributions as, for example, black holes.

References

- [1] M. Morris and K. Thorne. *Am. Jou. Phys.* **56**, 395 (1988)
- [2] M. Morris, K. Thorne and U. Yurtsever. *Phys. Rev. Lett.* **61**, 1446 (1988)
- [3] M. Visser. *Lorentzian Wormholes: From Einstein to Hawking*. American Institute of Physics. New York. (1995)
- [4] J. Lemos, F. Lobo y S. Quinet. *Morris-Thorne Wormholes with a Cosmological Constant*. *Phys. Rev.* **D68** 064004 (2003)
- [5] J.G. Cramer, R.L. Forward, M.S. Morris, M. Visser, G. Benford y G.A. Landis. *Natural Wormholes as Gravitational Lenses*. *Phys. Rev.* **D51**, 3117 (1995)
- [6] M. Safanova, D.F. Torres y G.E. Romero. *Microlensing by Natural Wormholes: Theory and Simulations*. *Phys. Rev.* **D65**, 023001 (2002)
- [7] V. Bozza. *Gravitational Lensing in the Strong Field Limit*. *Phys. Rev.* **D66**, 103001 (2002)
- [8] K.S. Virbhadra and G.F.R. Ellis. *Phys. Rev.* **D62**, 084003 (2000)

- [9] K.S. Virbhadra, D. Narasimha and S. M. Chitre. *Role of the scalar field in gravitational lensing*. *Astronomy and Astrophysics*. **337**, 1-8 (1998). astro-ph/9801174 [astro-ph]